Supporting Information

Multifunctional cardanol-based room-temperature phosphorescent material with multi-stimulus-responsive shape-memory for anti-Counterfeiting and encryption

Caiying Bo[a], Yiran Fu[a,b], Miao Li[a], Lihong Hu[a*], Meng Zhang[a*], Fei Song[a], Yonghong Zhou[a*]*

[a]Institute of Chemical Industry of Forest Products, CAF; national Engineering Research Centerfor Low-Carbon Processing and Utilization of Forest Biomass, Key Lab. Of Biomass Energy and Material, Jiangsu Province, Jiangsu Co-Innovation Center of Efficient Processing and Utilization of Forest Resources, Nanjing 210042, People's Republic of China

[b]College of Materials Science and Engineering, Nanjing Forestry University, Nanjing 210037, People's Republic of China.

[*] Corresponding authors. E-mail: newstar2002@163.com (Caiying Bo), ORCID: 0000-0002-7032-9931; hlh@icifp.cn (Lihong Hu); zhangmeng@icifp.cn (Meng Zhang); zyh@icifp.cn (Yonghong Zhou)

Contents

1. Experimental section

1.1. Materials

Cardanol (~ 95%, Cardolite chemical Co., Ltd.), 3-Aminobenzeneboronic acid (Shanghai Macklin Biochemical Co., Ltd.) N, N-Bis(2-hydroxyethyl) ethylenediamine (98%, Wuhan Xinweiye Chemical Co., Ltd), N, N,N',N'-tetrakis(2-hydroxyethyl)ethylenediamine(99%, Macklin). All other chemicals and reagents were reagent grade and used without further purification in this study.

1.2. Characterization

1.2.1. Fourier transform infrared spectroscopy analysis (FT-IR)

The FT-IR spectra were acquired on a Nicolet iS50 FTIR meter (Nicolet Instrument Crop., USA).

1.2.2. Nuclear magnetic resonance analysis (NMR)

^{1}H nuclear magnetic resonance (NMR) spectra of samples in d-DMSO were recorded on a Bruker AV-300 Advance NMR spectrometer (Bruker Corporation, Germany) at 300 MHz

1.2.3. Thermogravimetric Analysis (TGA)

TGA was carried out on a STA 209F1 thermogravimetry instrument (Netzsch Corporation, Germany) within a temperature from 40 °C to 600 °C under N_2.

1.2.4. Photoluminescence excitation (PLE) and photoluminescence (PL) analysis

Photoluminescence excitation, prompt emission and delayed emission spectra were measured on a FLS1000 fluorescence spectrophotometer (Edinburgh Instruments) under ambient condition.

1.2.5. General reprocessing procedure

The samples were first cut completely into fragments and then compressed at hot 80 °C, 10 MPa for 10 min. After cooling to room temperature, a recycled film was obtained.

1.2.6. Mechanical property

Mechanical property values were presented as the mean and standard deviation based on at least three trials using an UTM6503 instrument.

1.2.7. Shape memory

Shape-memory behavior testing: The thermally-induced shape memory behaviors were determined by thermo-mechanical analysis were conducted on DMA800 according to the procedure described in ref [1-2]. All samples were cut in rectangular pieces of approximately 10 mm×6.0 mm×0.5 mm. First, the samples were heated to programming temperature T_{prog} at the rate of 3 °C/min and held for 5 min before being stretched to the maximum stress. Then, while keeping a constant stress, they were rapidly cooled to below transition temperature T_{low} at 3 °C/min and held for 5 min. Finally, the stress was released to recovery temperature T_{rec} at 3 °C/min for triggering the shape recovery. The most significant parameters to evaluate the shape memory performance are the shape-recovery ratio (R_r) and shape-fixity ratio (R_f). They can be calculated by the following equations:

$$R_r = \frac{\varepsilon_{u(N)} - \varepsilon_{p(N)}}{\varepsilon_{u(N)} - \varepsilon_{p(N-1)}} \times 100 \quad \text{(S1)}$$

$$R_f = \frac{\varepsilon_{u(N)} - \varepsilon_{p(N-1)}}{\varepsilon_{m(N)} - \varepsilon_{p(N-1)}} \times 100 \quad \text{(S2)}$$

Where ε_u represents the strain after unloading, ε_p is the permanent strain after the shape recovery, and ε_m represents the maximum strain during loading. N in the equation denotes the cycle number.

IR light induced shape recovery: The samples were exposed to the irradiation of IR light at 1.8 W/cm², and the photothermal behavior have been investigated using a FLIR Pro thermal imaging camera.

1.2.8. Dynamic mechanical analysis (DMA)

DMA was performed on a Q800 solids analyzer (TA Corporation, USA) from -50 ºC to 150 ºC (3 °C/min, 1Hz). Cross-link density (v_e) values of the cured materials can be calculated using the following equation[3]:

$$v_e = \frac{E}{3RT} \quad \text{(S3)}$$

Where E is the storage modulus at rubbery states (T_g+20 °C), R is the gas constant (8.314 J/(mol·K)) and T is the Kelvin temperature of T_g+ 20°C.

1.2.9. Swelling tests

Samples were immersed in H_2O, 1 mol/L NaOH, 1 mol/L HCl, hexane (HEX), EtOH, DMF, THF, acetonitrile (ACN), dichloromethane (DCM), ethyl

acetate (ACE), and toluene (TOL) for different times at ambient temperature.

$$Swelling\ ratio\ (\%) = \frac{m_s - m_i}{m_i} \times 100 \quad \text{(S4)}$$

$$Insoluble\ fraction\ (\%) = 1 - \frac{m_i - m_d}{m_i} \times 100 \quad \text{(S5)}$$

Where m_i, m_s and m_d represent the weight of initial, swollen, and dry samples.

1.2.10. Self-healing tests

The Self-healing tests of the materials were tested by Leica optical microscope (Germany, ICC50 W). The self-healing efficiency was calculated using the ratio of the reduced scratch width to the initial scratch width of the materials.

1.2.11. Stress relaxation

The stress relaxation curves of the samples were conducted by DMA Q800 instrument with a strain value of 2% in "stress relaxation" mode. The activation energy (E_a) of the cured materials was calculated using the following equations [4-5]

$$\ln\tau^* = \frac{E_a}{RT} - \ln A \quad \text{(S 6)}$$

Where T is the absolute temperature, A is a pre-exponential factor, and R is the gas constant.

1.3. Synthetic Procedure

1.3.1. Synthesis of card polyphenol glycidyl ether (CPGE)

45 g (~0.15 mol) of cardanol was added in a four-necked round-bottom flask equipped with a mechanical stirrer, thermometer sensor, and reflux condenser; then, 141.17g (1.5 mol) of phenol was added into the flask, followed by addition of 1.86 g of tetrafluoro boric acid. The resultant solution was allowed to react at 90 °C for 2 h. After the reaction was complete, the crude product was filtered and washed with excessive hot H_2O. Finally, the organic phase was dried with anhydrous $MgSO_4$ and then filtered. Typically, card polyphenol reacted with epichlorohydrin under alkaline conditions to form card polyphenol glycidyl ether, The epoxy value of CPGE was 0.193 mol/ 100 g.

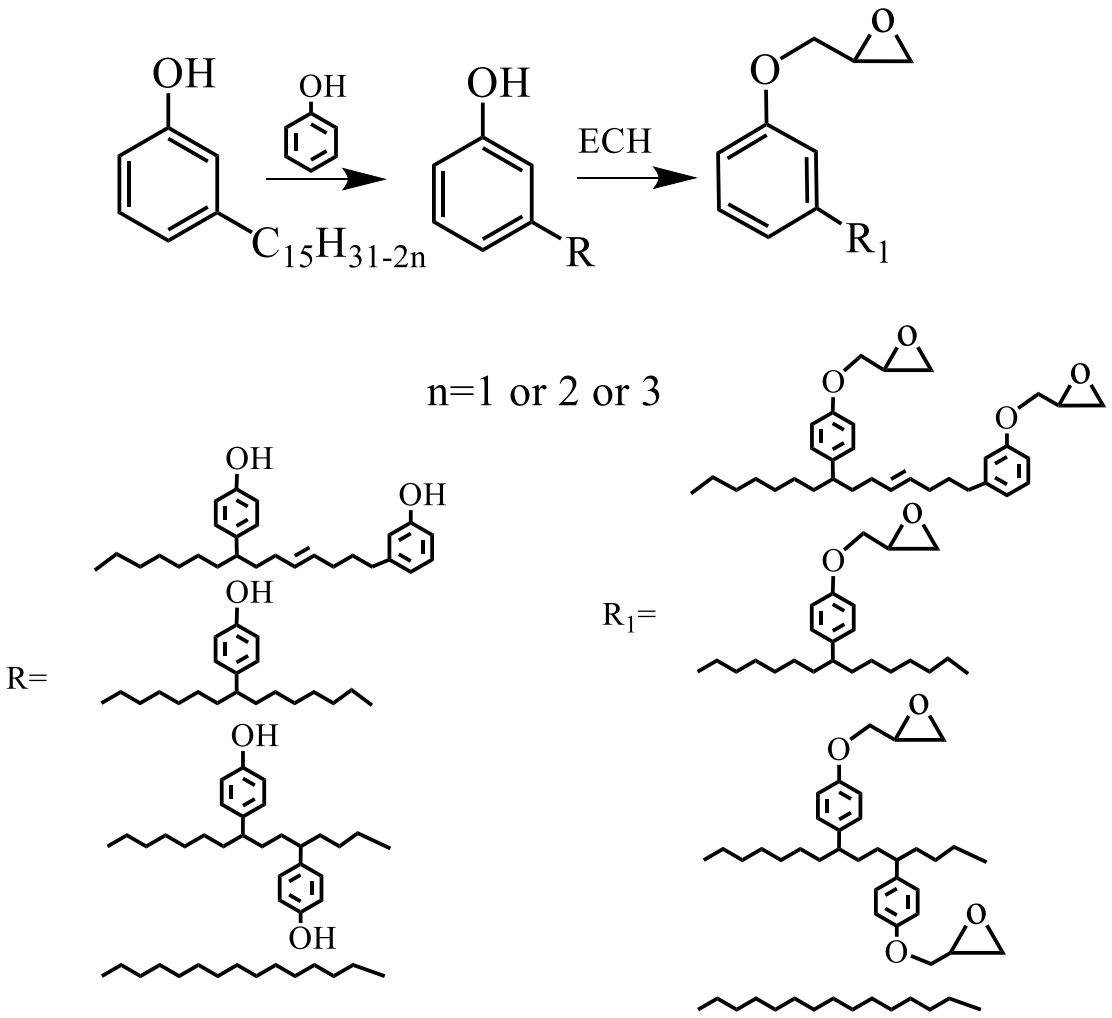

Scheme S1. Synthesis route of CPGE

1.3.2. Synthesis of N-coordinated bicyclic boronic ester amine compounds (BNAs)

Synthesis of BNA-1: N,N-Bis(2-hydroxyethyl)ethylenediamine (7.78 g, 52.50 mmol) and 3-aminobenzeneboronic acid (6.85 g，50 mmol) were mixed and dissolved in DMF (100 mL) at 40 ℃, and the mixture was stirred for 1 h. The resulting mixture was reduced in volume by rotary evaporation under reduced pressure. Then a white powder product with the yield of 82 % was obtained after washing.

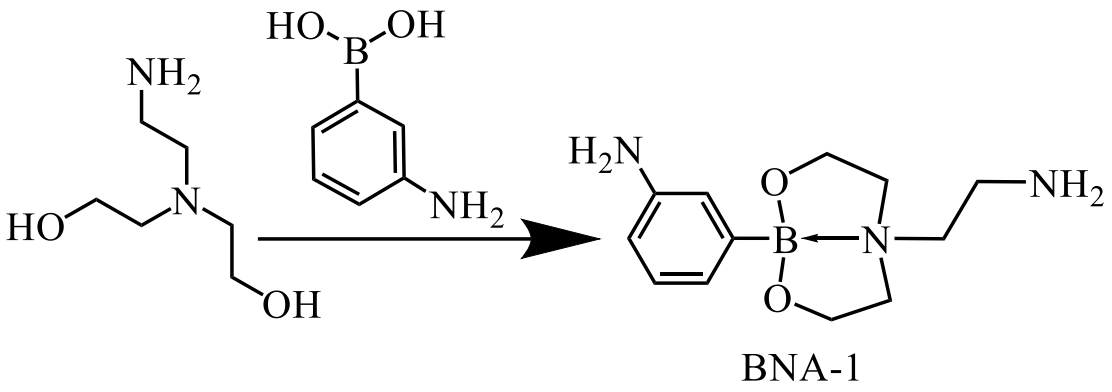

Scheme S2. Synthesis route of BNA-1

Synthesis of BNA-2: N,N,N',N'-tetrakis(2-hydroxyethyl)ethylenediamine (6.20g, 26.24 mmol) and 3-aminobenzeneboronic acid (6.85g，50 mmol) were mixed and dissolved in DMF (100 mL) at 40 ℃, and the mixture was stirred for 1 h. The resulting mixture was reduced in volume by rotary evaporation under reduced pressure. Then a white powder product with the yield of 80 % was obtained after washing.

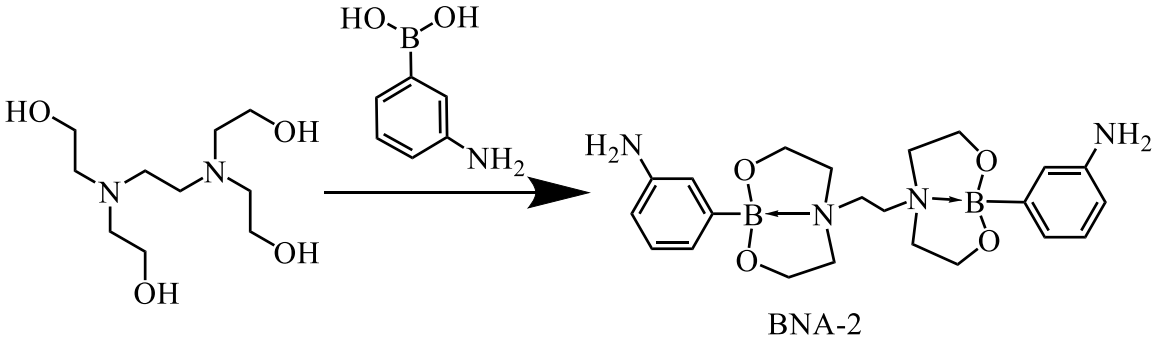

Scheme S3. Synthesis route of BNA-2

1.3.3. Preparation of cardanol-based epoxy resin CPGE-BNAs

As shown in Scheme S4, a certain amount of CPGE and BNAs were dissolved in 10 mL DMF. The obtained solutions were stirred at 120 °C for 7 h and dried at 80 °C in vacuum oven remove the DMF to make a smooth film. By changing the molar ratios of epoxy and amino group (0.8, 1.0, 1.2, 1.5, 1.8 and 2.0 respectively), the obtained CPGE-BNA1 were named as CPGE-BNA1-0.8, CPGE-BNA1-1.0, CPGE-BNA1-1.2 and CPGE-BNA1-1.5, respectively. Epoxy resin CPGE-BNA2 was name through the same method.

2. Results and Discussion

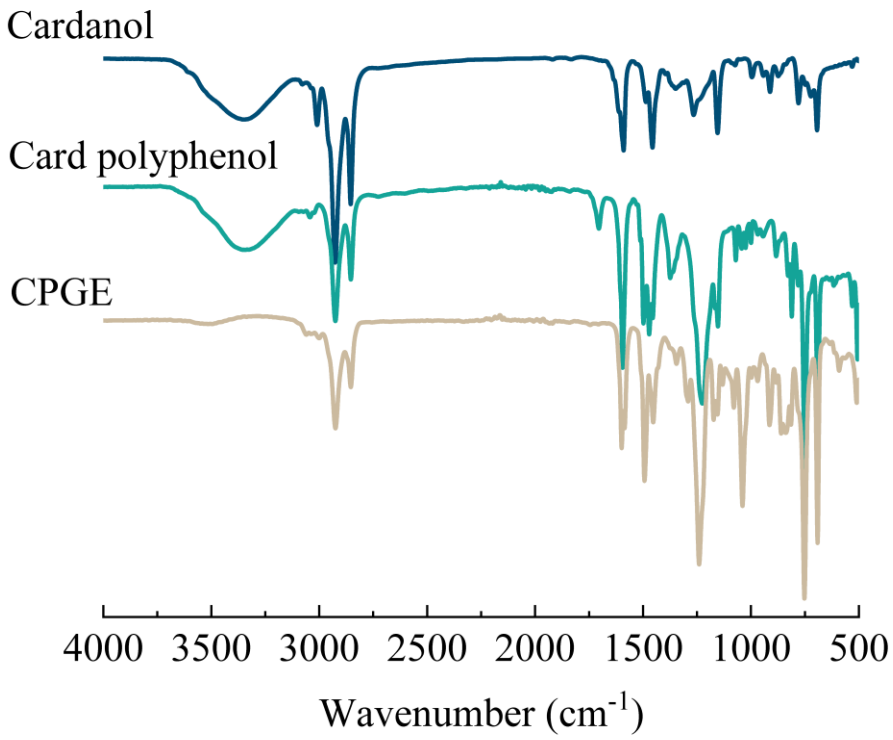

Figure S1. FT-IR spectra of cardanol, card polyphenol and CPGE

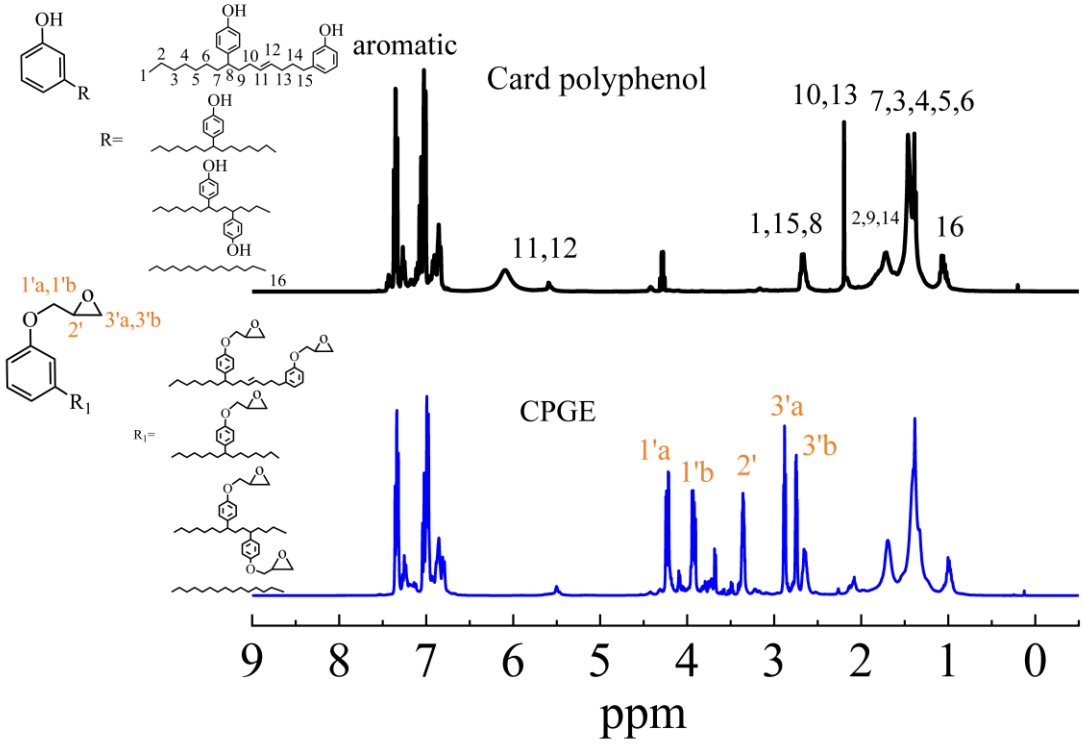

Figure S2. ^{1}H NMR spectra of card polyphenol and CPGE

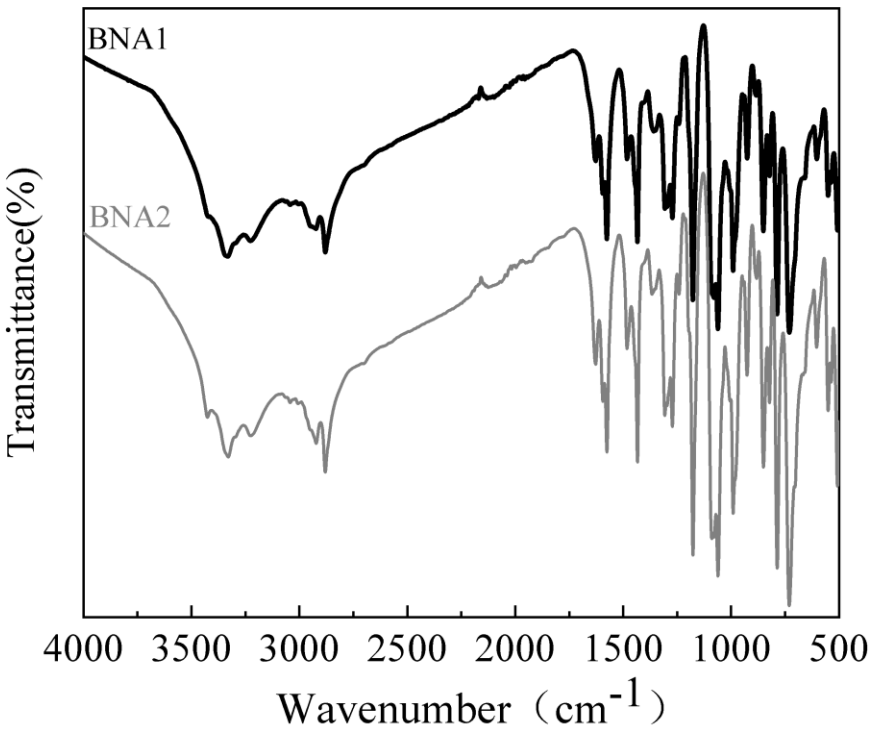

Figure S3. FT-IR spectra of BNA1 and BNA2

In the FT-IR spectra, BNAs show the characteristic absorption bands of typical boronic esters: 1454,1357,1240, 1307, 1040 [6].

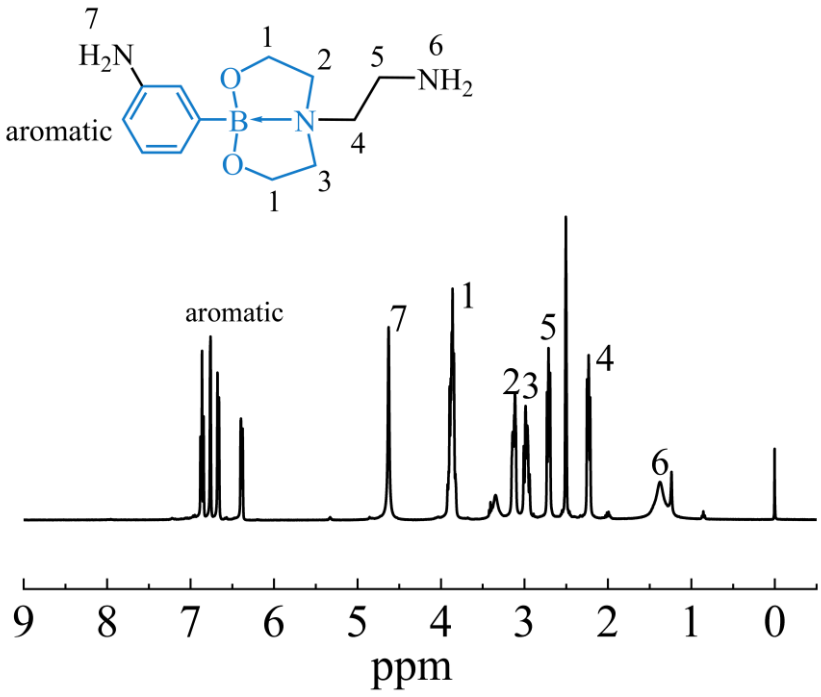

Figure S4. ^{1}H NMR spectra of BNA1

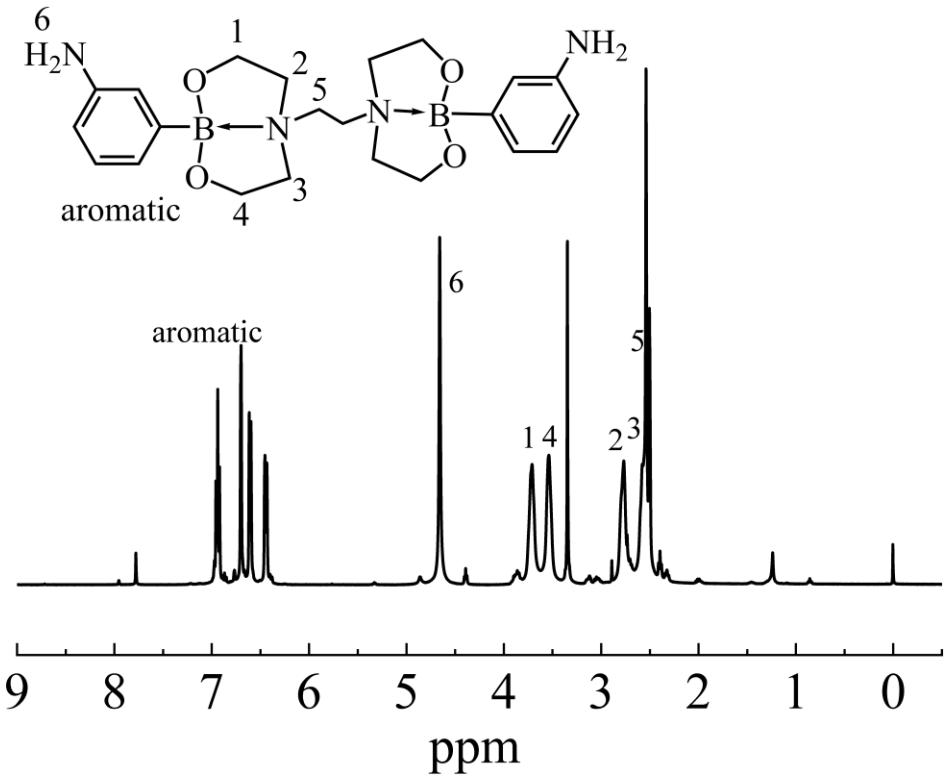

Figure S5. ^{1}H NMR spectra of BNA2

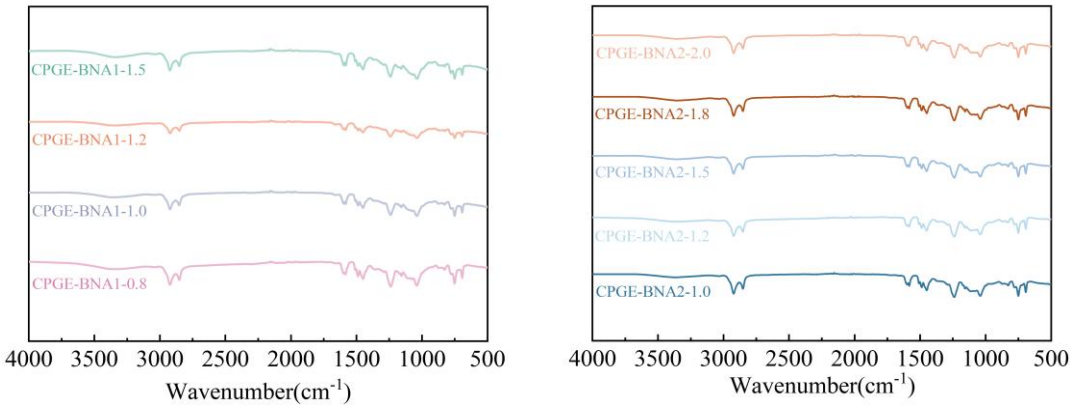

Figure S6. FT-IR spectra of CPGE-BNAs

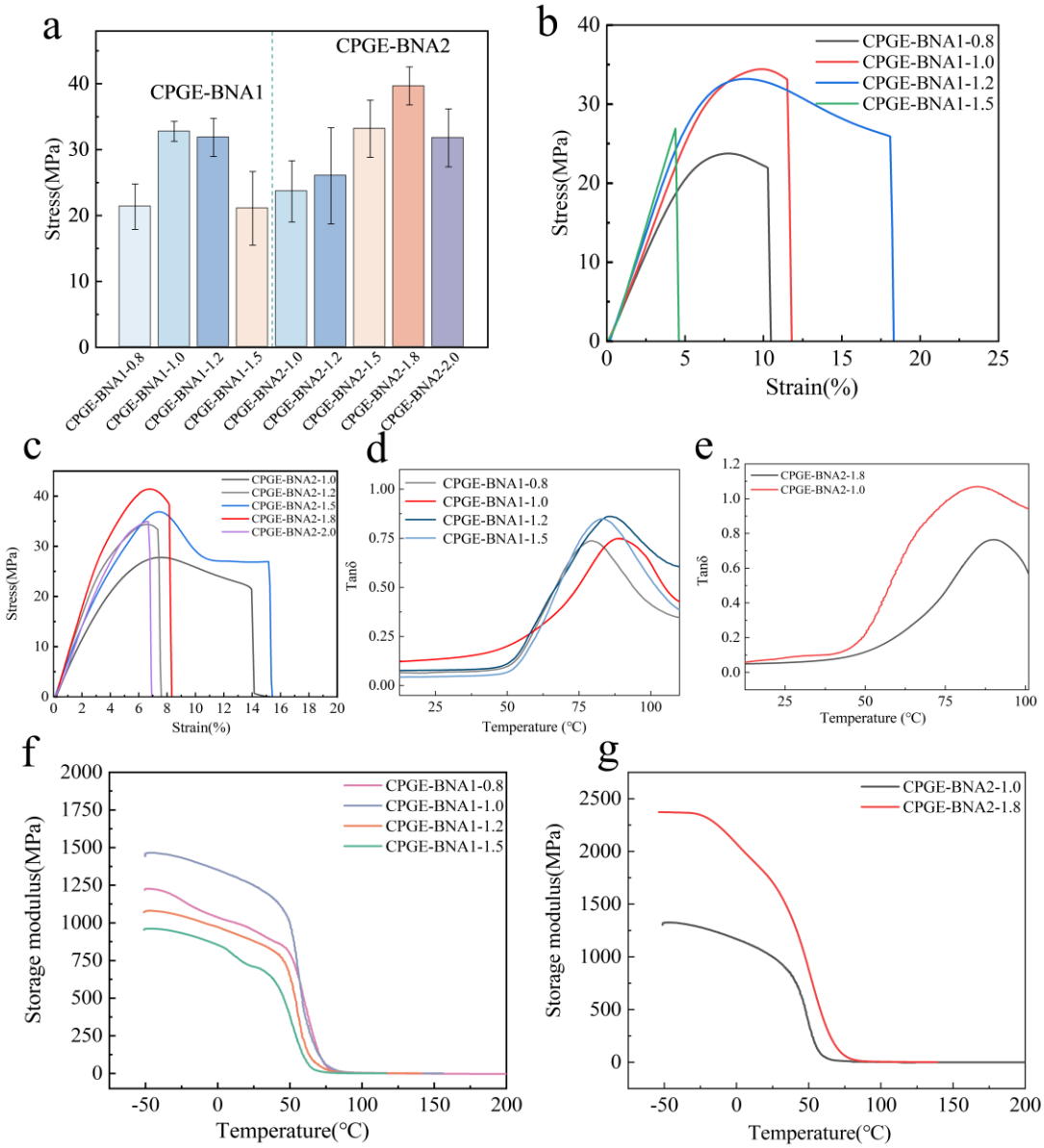

Figure S7. (a)The mechanical properties, (b,c) stress–strain curves of CPGE-BNA1 and CPGE-BNA2, (d,e) tan δ and (f,g) *E* of CPGE-BNA1 and CPGE-BNA2

Table S1 Mechanical and thermal properties of CPGE-BNA1 and CPGE-BNA2

Sample	Tensile Strength (MPa)	T_g (°C)	E'$_{25}$ (MPa)	ν_e (10^3mol/m^3)
CPGE-BNA1-0.8	21.35±3.45	78.99	949	0.16
CPGE-BNA1-1.0	32.77±1.51	88.97	1249	0.33
CPGE-BNA1-1.2	31.86±2.89	84.80	878	0.24
CPGE-BNA1-1.5	21.09±5.58	82.45	711	0.05
CPGE-BNA2-1.0	23.67±4.64	83.49	998	0.20
CPGE-BNA2-1.2	26.03±7.30	—	—	
CPGE-BNA2-1.5	33.17±4.33	—	—	
CPGE-BNA2-1.8	39.67±2.88	89.72	1700	0.34
CPGE-BNA2-2.0	31.79±4.40	—	—	

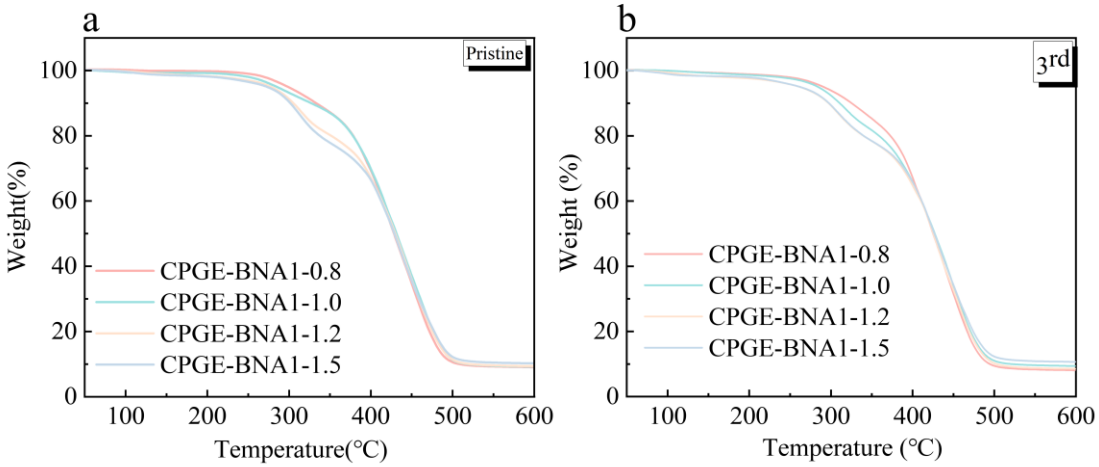

Figure S8. TGA of original and 3rd reprocessed CPGE-BNA1

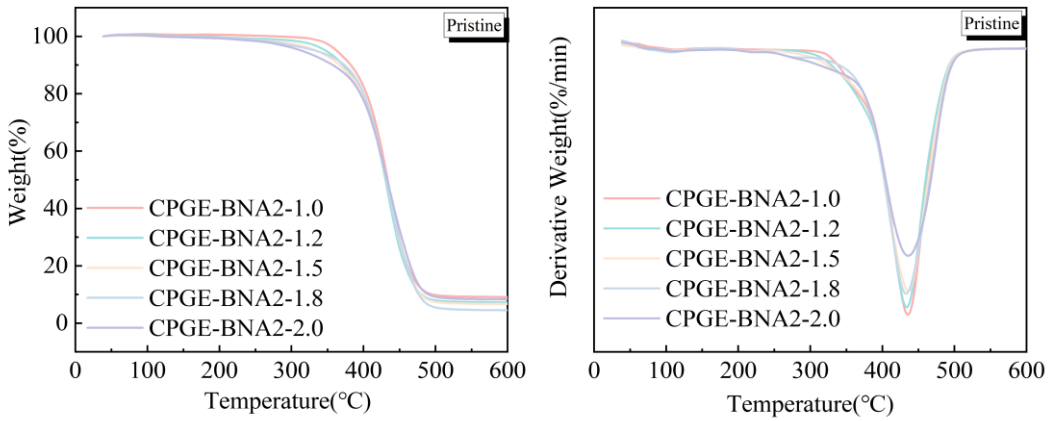

Figure S9. TGA and DTG of CPGE-BNA2

Table S2 Thermal degradation results of original and 3rd reprocessed CPGE-BNA1

Sample		$T_{-5\%}$ (℃)	T_{max} (℃)		Char yield (%)
			I	II	
CPGE-BNA1-0.8	pristine	297.89		437.48	9.09
	3rd	290.65		439.40	8.10
CPGE-BNA1-1.0	pristine	284.81	311.71	443.63	9.26
	3rd	283.93	317.93	449.93	9.41
CPGE-BNA1-1.2	pristine	277.85	312.96	436.23	9.37
	3rd	261.11	308.11	430.11	8.56
CPGE-BNA1-1.5	pristine	271.91	290.26	444.76	10.25
	3rd	262.11	309.11	435.11	10.68

Table S3 Thermal degradation results of CPGE-BNA2

Sample	$T_{-5\%}$(℃)	T_{max} (℃)	Char yield (%)
CPGE-BNA2-1.0	362.53	435.53	9.12
CPGE-BNA2-1.2	347.85	433.85	7.24
CPGE-BNA2-1.5	334.89	435.89	6.69
CPGE-BNA2-1.8	332.85	432.85	4.49
CPGE-BNA2-2.0	313.86	435.86	8.30

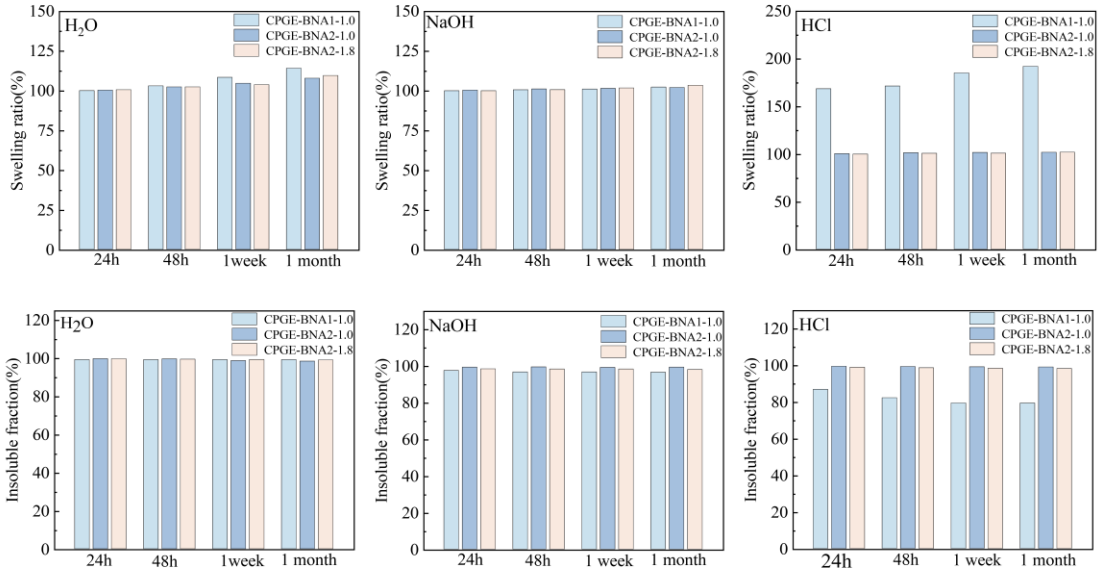

Figure S10. Swelling ratio and insoluble fraction for CPGE-BNA1-1.0, CPGE-BNA2-1.0, and CPGE-BNA2-1.8 in H_2O, NaOH, and HCl at different times

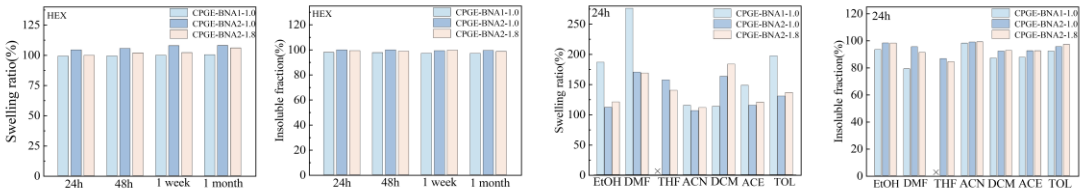

Figure S11. Swelling ratio and insoluble fraction for CPGE-BNA1-1.0, CPGE-BNA2-1.0, and CPGE-BNA2-1.8 in different solvents at different times

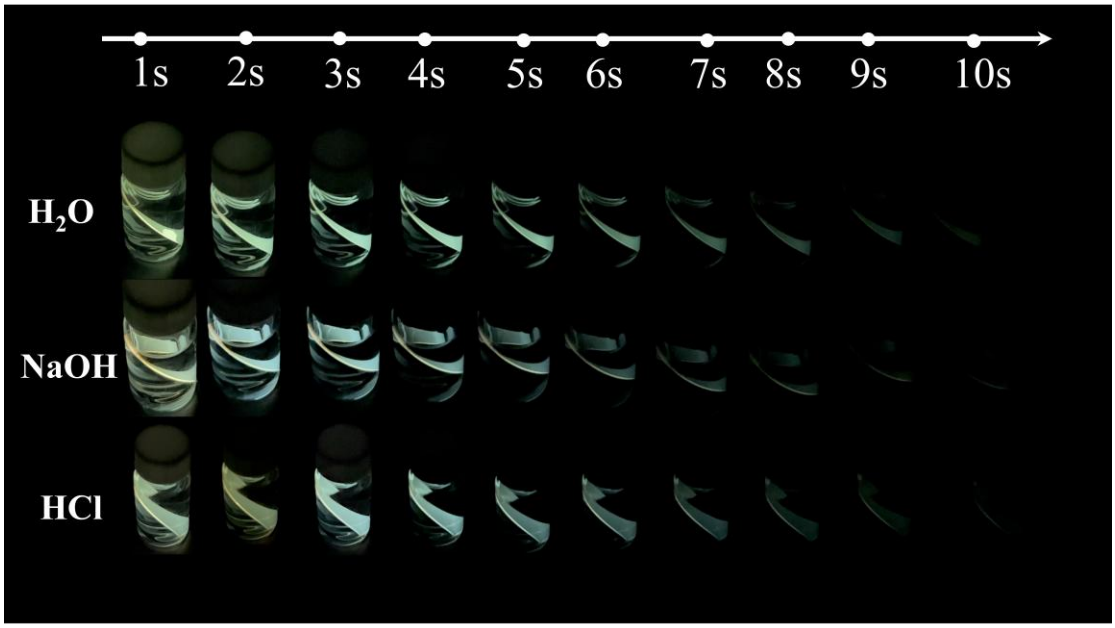

Figure S12. Afterglow images of CPGE-BNA2-1.0 excited at 365 nm immersed in H_2O, HCl, NaOH for four weeks

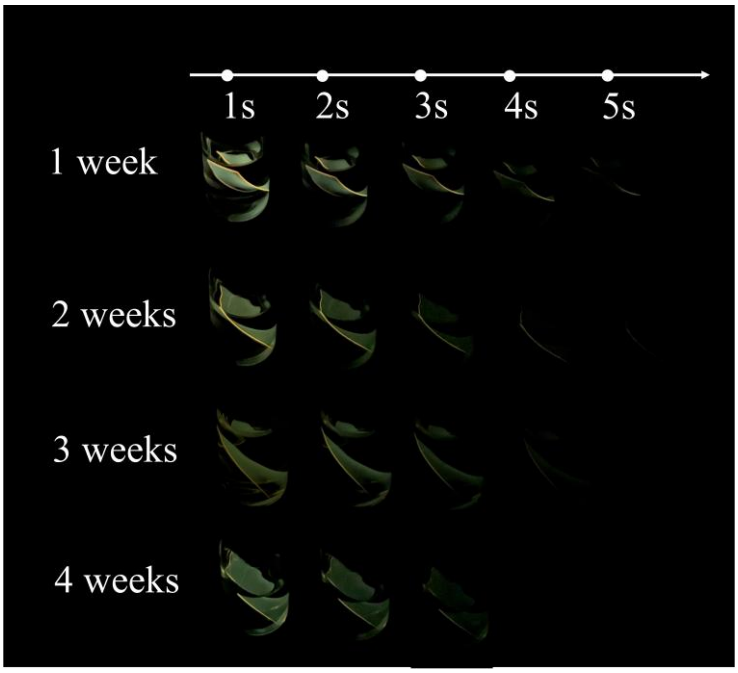

Figure S13. Afterglow images of CPGE-BNA2-1.0 excited at 365 nm in hexane at different times

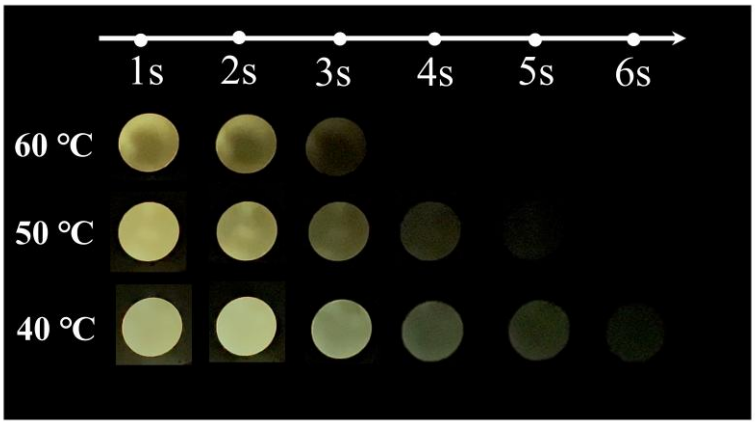

Figure S14. Afterglow images of CPGE-BNA2-1.0 excited at 365 nm at different temperatures

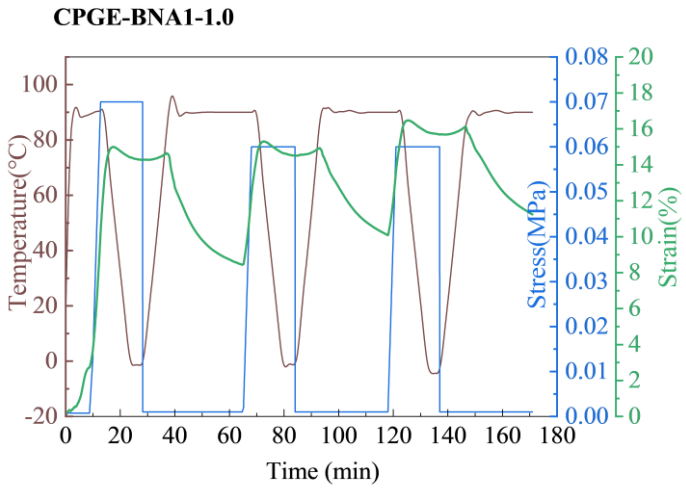

Figure S15. Consecutive shape memory cycles of CPGE-BNA1-1.0

Table S4 Shape fixity and recovery properties of CPGE-BNA1-1.0, CPGE-BNA2-1.0 and CPGE-BNA2-1.8

	Cycle	CPGE-BNA1-1.0 (%)	CPGE-BNA2-1.0 (%)	CPGE-BNA2-1.8 (%)
	1	97.73	96.66	96.81
R_f	2	97.52	96.42	96.77
	3	97.94	97.70	96.76
	1	53.48	87.75	95.84
R_r	2	75.91	91.57	97.40
	3	82.10	~100	~100

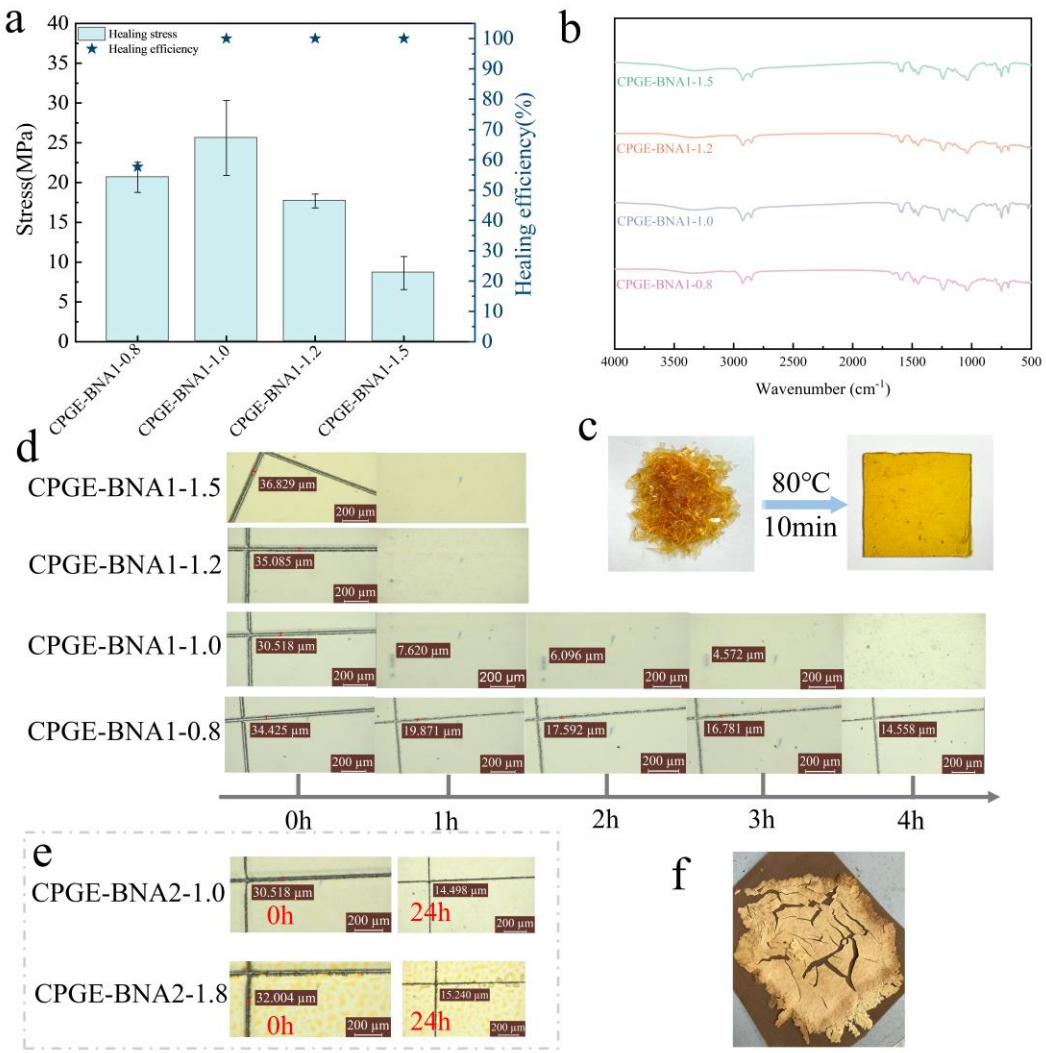

Figure S16. Recyclability and self-healing of CPGE-BNA1 system polymers: (a) Healing efficiency and mechanical properties of the recycled CPGE-BNA1 polymers after hot processing. (b) FT-IR spectra. (c) Images recording the reprocessing of CPGE-BNA1 system polymers from fractured pieces into a new film via thermal processing. (d) Scratch-repairing images of the CPGE-BNA1 system polymers. (e) Scratch-repairing images of the CPGE-BNA2-1.0 and CPGE-BNA2-1.8. (f) Images recording the reprocessing of CPGE-BNA2-1.0 from fractured pieces.

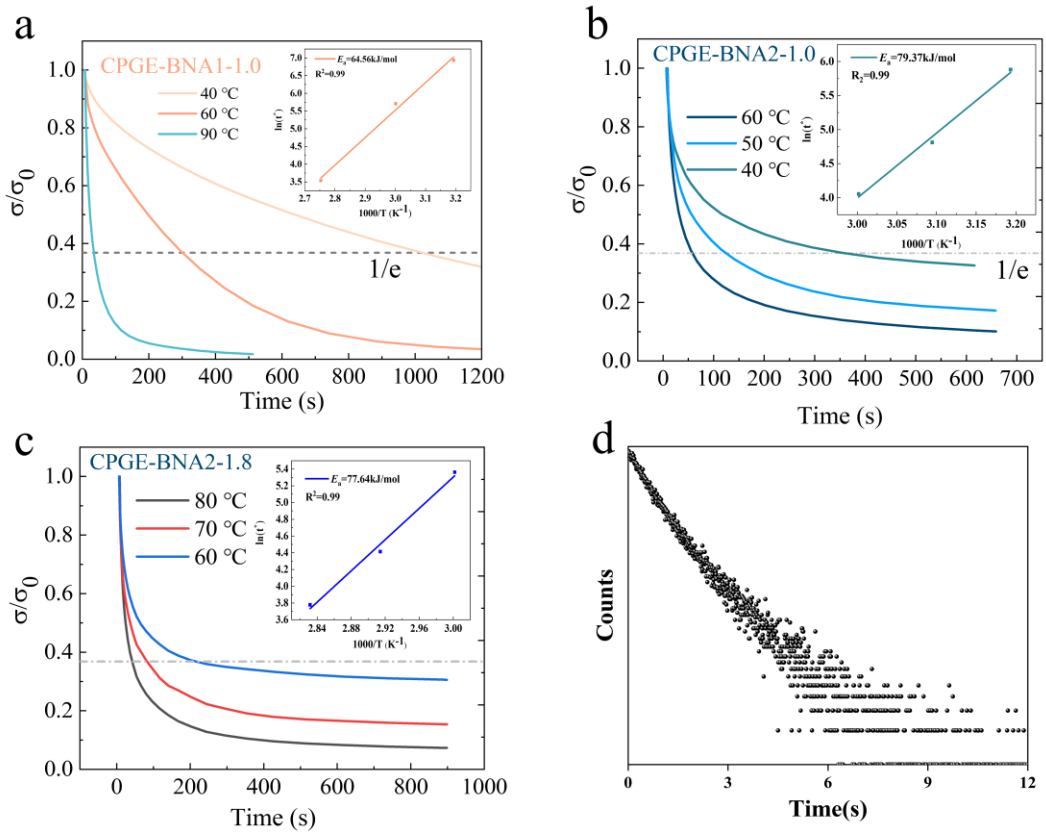

Figure S17. Stress relaxation curves and the relationship between ln(τ*) and temperature: (a) CPGE-BNA1-1.0, (b) CPGE-BNA2-1.0 and (c) CPGE-BNA2-1.8 at different temperatures. (d) Time-resolved emission-decay curves of reprocessed CPGE-BNA1-1.0, excited at 365 nm.

References

1 C. Bo, Y. Sha, F. Song, M. Zhang, L. Hu, P. Jia, Y. Zhou, *Journal of Cleaner Production.* 2022, **341**.

2 C. Bo, S. Guo, Y. Sha, L. Yuan, L. Hu, P. Jia, Y. Zhou, G. Feng, M. Zhang, *Composites Science and Technology.* 2022, **230**.

3 Y. Liu, S. Ma, Q. Li, S. Wang, K. Huang, X. Xu, B. Wang, J. Zhu, *European Polymer Journal.* 2020, **135**.

4 C. Hao, T. Liu, S. Zhang, L. Brown, R. Li, J. Xin, T. Zhong, L. Jiang, J. Zhang, *ChemSusChem.* 2019, **12**, 1049-1058.

5 H. Memon, H. Liu, M. A. Rashid, L. Chen, Q. Jiang, L. Zhang, Y. Wei, W. Liu, Y. Qiu, *Macromolecules.* 2020, **53**, 621-630.

6 H. Kang, W. Wei, L. Sun, R. Yu, E. Yang, X. Wu, H. Dai, *Chemistry of Materials.* 2023, **35**, 2408-2420.